Surface Science 163 (1985) 503–515
North-Holland, Amsterdam

ELECTRONIC MODEL FOR ENERGIES, RELAXATIONS AND RECONSTRUCTION TRENDS AT METAL SURFACES

D. TOMÁNEK and K.H. BENNEMANN

Institut für Theoretische Physik, Freie Universität Berlin, Arnimallee 14, D-1000 Berlin 33, Germany

Received 8 March 1985; accepted for publication 7 June 1985

Surface energies and relaxations are calculated within the tight-binding formalism and including also repulsive interatomic interactions. At fcc and bcc metal surfaces we obtain damped oscillatory multilayer relaxations. Furthermore, we present results for the reconstruction at clean (110) and (100) surfaces of Ir, Pt and Au. CO-suppressed and H-induced reconstruction observed at some transition metal surfaces is quantitatively explained by coverage-dependent correction terms to surface energies.

1. Introduction

The equilibrium geometry at transition metal surfaces is presently studied intensively [1]. Similar relaxations and reconstruction patterns have been observed on surfaces of different metals by means of low-energy electron difraction [2–13] (LEED), He- and X-ray diffraction [14–16], ion scattering spectroscopy [17], scanning tunneling microscopy [18,19] and transmission electron microscopy [20]. Despite successful calculations of the relaxations on simple metal surfaces [21] and of the reconstruction on few transition metal surfaces [22], one still lacks a general understanding of the main physical factors determining the surface geometry. Only recently, theoretical calculations attempted to account for the universal behaviour of surface and interface energies [23,24]. Thus, it is the main objective of this paper to show that the similar relaxation and reconstruction behaviour observed at many transition metal surfaces can be described within a simple general framework.

The paper is organized as follows. In section 2 we present a simple criterion for the reconstruction at clean and adsorbate-covered surfaces and a tight-binding-type electronic theory for surface energies and atomic relaxations. In section 3 we use this theory to calculate the surface relaxations and the most favourable reconstruction patterns for several clean transition metal surfaces. Furthermore, we investigate the CO-suppressed Pt(100)-(hex) reconstruction and the H-induced Ni and Pd(110)-(1 × 2) reconstruction. In section 4 we present a discussion and a generalization of our results.

0039-6028/85/$03.30

2. Theory

Surface reconstruction is a result of the minimization of the surface free energy, which at $T = 0$ K reduces to the surface tension γ given by

$$\gamma = \frac{1}{N_S} \sum_{i}^{N_{tot}} \left[E_{coh}(\text{bulk}) - E_{coh}(i) \right]. \tag{1}$$

Here, N_S (N_{tot}) is the number of surface atoms (total number of atoms) in the crystal and $E_{coh}(i)$ denotes the atomic binding energy of an atom at site i. The heat of reconstruction at a clean surface $\Delta\gamma_R^0$ is given by the difference of the surface tensions γ_R^0 and γ_U^0 of the reconstructed and unreconstructed surface, respectively, as

$$\Delta\gamma_R^0 = \gamma_R^0 - \gamma_U^0. \tag{2}$$

In the presence of adsorbates the heat of reconstruction is given by

$$\Delta\gamma_R = \Delta\gamma_R^0 - \Delta\gamma^{ads}, \tag{3}$$

where

$$\Delta\gamma^{ads} = \theta(E_{ads,R} - E_{ads,U}). \tag{4}$$

Here, E_{ads} is the adsorption bond energy and θ the coverage. The changes $(E_{ads,R} - E_{ads,U})$ can be obtained from the experiment or an accurate calculation. Using eq. (4), we obtain a general criterion for reconstruction at $T = 0$ K,

$$\Delta\gamma_R = \Delta\gamma_R^0 - \Delta\gamma^{ads} < 0. \tag{5}$$

This criterion can be used to calculate the adsorbate-induced or -suppressed reconstruction, as shown schematically in fig. 1.

In order to calculate the surface tension γ^0 from eq. (1) we decompose the atomic binding energy $E_{coh}(i)$ into an attractive band structure and a repulsive Born–Mayer part [24,25]. The model assumption of a single-band solid, local charge neutrality and the same band shape (except for a re-scaled bandwidth) at each site allows us to relate the band structure energy at each site to the bulk value without assuming a model (rectangular, Gaussian) density of states [25]. Then [24,25],

$$E_{coh}(i) = \frac{E_{coh}(\text{bulk})}{(1 - q/p)(Z_{bulk})^{1/2}} \left[\left(\sum_j{}' \exp\left[-2q(r_{ij}/r_0 - 1) \right] \right)^{1/2} - \frac{1}{(Z_{bulk})^{1/2}} \frac{q}{p} \sum_j{}' \exp\left[-p(r_{ij}/r_0 - 1) \right] \right]. \tag{6}$$

Here, the summations extend over the nearest neighbours of i, r_{ij} (r_0) denote the respective (bulk equilibrium) distances and Z_{bulk} is the bulk coordination

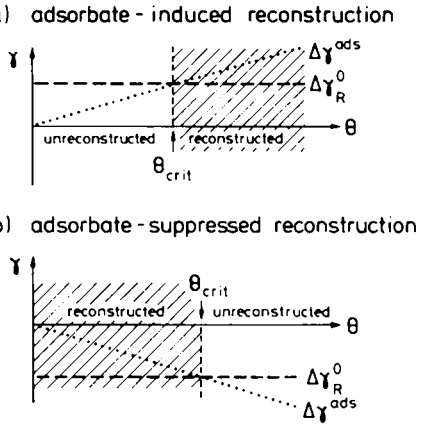

Fig. 1. Illustration of adsorbate-induced and -suppressed reconstruction trends.

number. q and p describe the distance dependence of the hopping integrals and Born–Mayer interactions, respectively, and are related to bulk elastic properties. Clearly, eq. (6) will correctly describe reconstruction trends only in cases where mainly the close-packing of the topmost layer, rather than details in the electronic structure, is the driving force for reconstruction.

Surface relaxations can be obtained from minimizing the surface energy

$$\partial\gamma^0/\partial r_{1,j} = 0 \tag{7}$$

with respect to atomic positions.

From eq. (6) it is obvious that in our formulation surface relaxations depend purely on p and q. On the other hand, surface tensions γ^0 and heats of reconstruction scale (for constant p and q) with E_{coh}(bulk) and hence results obtained for one metal can easily be generalized to other systems.

3. Applications and numerical results

3.1. Relaxations at fcc and bcc surfaces

First, we apply our general simple theory to study multilayer relaxations at fcc and bcc surfaces. So far, the oscillatory relaxations generally observed at metal surfaces [2–7] have been calculated in free- and nearly-free-electron metals. While the predicted trends agreed with experiment, the absolute values showed a strong dependence on the electron density profile assumed [21].

We show that a surface contraction and oscillatory multilayer relaxations follow also from our energy expression, eq. (6). As can be inferred from fig. 2, for unrelaxed nearest-neighbour distances the repulsive part E_{R} of E_{coh} is

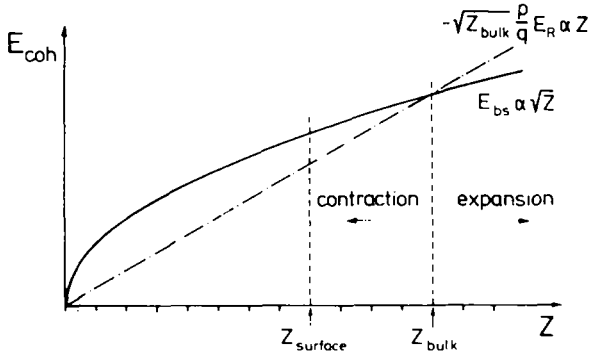

Fig. 2. Schematic decomposition of the atomic binding energy E_{coh} into attractive and repulsive parts E_{bs} and E_R, respectively, for unrelaxed nearest-neighbour distances. The consequences for oscillatory multilayer relaxations are discussed in section 3.1.

proportional to the coordination number Z, while the attractive part E_{bs} is proportional to $Z^{1/2}$. In the bulk attraction and repulsion are in equilibrium for unrelaxed distances. At the surface with a lower coordination number $Z_{surface} < Z_{bulk}$ the attractive part of E_{coh} outweighs the repulsion and induces a surface contraction. This contraction, however, simulates a higher coordination number $Z > Z_{bulk}$ in the second layer with full bulk coordination. In this region the repulsion outweighs the attraction and causes an expansion of the next interlayer distance. In this way a damped oscillatory relaxation is induced in the following layers.

We calculated relaxations at vertical interlayer distances Δd_{ij} and horizontal displacements Δy_i at Pt(110) and W(211) surfaces. For Pt we used [26] $E_{coh}(\text{bulk}) = 5.86$ eV, $r_0 = 2.77$ Å, and for the bulk modulus $B = 2.88 \times 10^{12}$ dyn/cm^2. This yields [24,26] $p = 11.1$ and $q = 3.7$. For W we assumed [24] $p = 9.8$, $q = 3.3$ and $r_0 = 2.74$ Å. Since in our model relaxations depend only on p and q and since these values are very similar in many transition metals [24], we do not expect strong material dependence on multilayer relaxations. The results of our calculation are presented in table 1 together with a compilation of experimental data for different materials. The damped oscillatory multilayer relaxations on fcc(110) surfaces and their expected universal behaviour, predicted on the basis of a model which uses only bulk metal properties as input, agree very well with observed relaxations.

At bcc(211) surfaces, which show some similarity with fcc(110) surfaces [7], damped oscillatory relaxations are predicted and observed [7] both perpendicular and parallel to the surface. As expected, the topmost interlayer spacing d_{12} contracts [7]. In contrast to the experiment, the horizontal shifts Δy_i of the individual layers (along the rows) differ in direction from those obseved [7] on the Fe(211) and predicted [21] for the Na(211) surfaces. We find a horizontal

Table 1
Calculated and experimental relaxations of the vertical interlayer distances Δd_{ij} and horizontal displacements Δy_i of the individual atomic layers i at fcc (110) and bcc (211) surfaces

System	Δd_{12} (%)	Δd_{23} (%)	Δd_{34} (%)	Δd_{45} (%)	Δy_1 (Å)	Δy_2 (Å)	Δy_3 (Å)	Δy_4 (Å)	Ref.
Pt(110) (theory)	−9.5	+1.7	−0.6	+0.3					Present work
Ni(110)	−8.4±0.8	+3.1±1.0	–	–					[2]
Cu(110)	−8.5±0.6	+2.3±0.8	−0.9±0.9	−0.8±0.9					[3]
Ag(110)	−7.8±2.5	+4.3±2.5	–	–					[4]
Al(110)	−8.5%	+5.5	+2.2	+1.6					[5]
	−8.6%	+5.0	−1.6	–					[6]
W(211) (theory)	−8.3	−1.5	+0.6		+0.12	−0.01	−0.00	−0.00	Present work
Fe(211)	−10.5	+5	−1		−0.24	+0.04			[7]

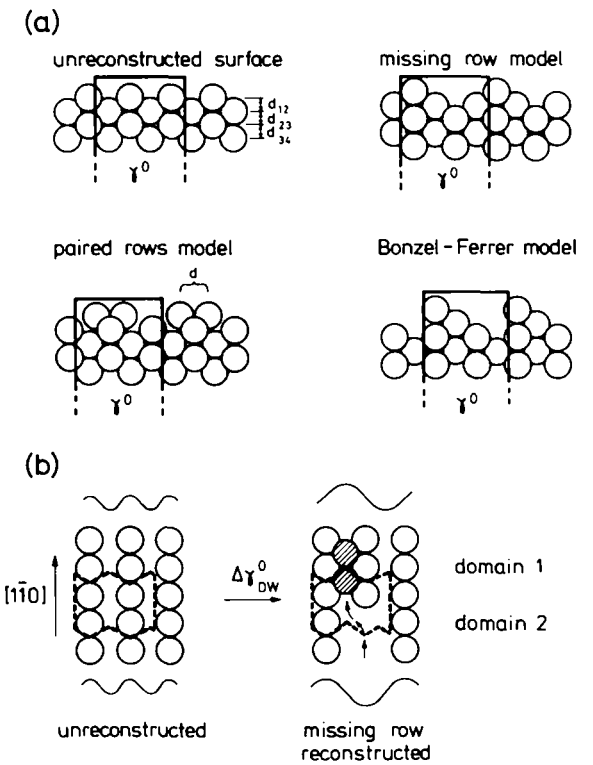

Fig. 3. (a) Side view of the unreconstructed and (1×2) reconstructed fcc(110) surfaces. The dashed line surrounds the surface area considered for the surface tension γ^0 given in table 2. (b) Top view of the domain wall formation mechanism for the missing row reconstruction proposed in ref. [18]. Dashed line surrounds the sites considered in the domain wall energy $\Delta\gamma^0_{DW}$.

Table 2
Calculated surface energies γ^0 of relaxed Pt(110), Pt(100) and Pt(111) surfaces for different reconstruction models

System	γ^0 (eV)	$\Delta\gamma_R^0$ (eV)
Pt(110)-(1×1)		
unreconstructed	1.84 [a]	
Pt(110)-(1×2)		
missing row	1.77 [a]	−0.04 [a]
Bonzel–Ferrer	2.53 [a]	+0.76 [a]
Pt(100)-(1×1)		
unreconstructed	0.69 [b,c]	
Pt(100)-(1×5)		
"bridge"	0.63 [c]	−0.06 [c]
"top"	0.64 [c]	0.05 [c]
Pt(100)-(hex)	0.60 [c]	−0.09 [c]
Pt(111)-(1×1)		
unreconstructed	0.43	

[a] The surface sites considered for γ^0 are shown in fig. 3a.
[b] Additional adatoms at the (100) surface account for the atom number conservation during the reconstruction.
[c] Average value per topmost-layer atom, irrespective of the surface Wigner–Seitz cell.

shift of the topmost layer toward higher symmetry with respect to the third-layer atoms located directly below and towards lower symmetry with respect to second-layer atoms located aside.

3.2. (1×2) reconstruction at clean Ir, Pt and Au(110) surfaces

The (1 × 2) reconstruction at the (110) surfaces of late 5d metals has been extensively investigated both experimentally [16–18,20,27] and theoretically [28]. Among the different models proposed for the (1 × 2) reconstruction, the missing row and partly the Bonzel–Ferrer model seem to be most in agreement with experiment [16–18,20,27]. An illustration of these models as well as of the unreconstructed surface is given in fig. 3a. The controversy about the long diffusion distances necessary to create a missing row surface [27] have been resolved by suggesting a domain formation mechanism [18], shown schematically in fig. 3b.

We calculated surface tensions and heats of reconstruction for the Pt(110)-(1 × 1) and (1 × 2) surfaces. Our results are presented in table 2. With respect to our former recursion technique calculation [28] the number of surface layers has been doubled and the number of inequivalent sites considered increased to 12. Oscillatory multilayer relaxations, similar to those shown in table 1, are obtained also on the reconstructed surfaces [29]. According to our results, the

missing row reconstruction is energetically slightly favoured at $T = 0$ K, while the Bonzel–Ferrer structure can be discarded on energetic grounds.

As shown in fig. 3b, the transition from the unreconstructed surface to a "missing row" structure is accompanied by the formation of energetically unfavourable domain walls. The domain wall formation energy $\Delta\gamma^0_{DW}$, defined by the change of γ^0 in the dashed area shown in fig. 3b, amounts to $\Delta\gamma^0_{DW} = 0.32$ eV for Pt. We conclude that the energy gain upon forming missing row domains of 10 and more atoms in the $[1\bar{1}0]$ direction already outweighs the energy cost of domain walls. Domain sizes of 10 and more atoms also seem to be consistent with experimental observation [18].

3.3. (hex) reconstruction at clean Ir, Pt and Au(100) surfaces

Despite detailed experimental investigations [8–10,14,19] of the surface structure at the (100) surfaces of Ir, Pt and Au, so far no theory exists to explain the observed complex reconstruction behaviour. The superstructures observed reach from Ir and Pt(100)-(1×5) with relatively simple unit cells [9,10] to the complex c(26×68) reconstruction at the Au(100) surface [8]. The common feature of these structures is a local (1×5) superstructure caused by hexagonal close packing and a uniaxial 4% contraction within the topmost layer [8,14,19]. Structure models are presented in fig. 4a. More complex "hex" structures are obtained by assuming isotropic contractions and slight rotations of the topmost layer by $\varphi < 1°$. It should be noted that the close-packed reconstructed surface contains $\approx 20\%$ more atoms than the unreconstructed surface, which must also be considered in energy calculations.

Here, we present a calculation of the surface tension and relaxations at Pt(100) surfaces. Results are presented in table 2 and figs. 4 and 5. Very similar p and q values in Ir and Au allow a generalization of the Pt results to these metals, since γ^0 scales with E_{coh}(bulk). The (hex) reconstruction occurs if the decrease in surface tension upon close packing the topmost layer (compare the surface tensions of unreconstructed Pt(100) and Pt(111) surfaces in table 2) outweighs the misregistry energy with the underlying layers.

In our calculation we first assumed the close-packed rows of the top hexagonal close-packed layer to be commensurate with the substrate in the [011] direction (fig. 4a), which allowed for a "top" or a "bridge" registry [8,19]. The relaxed surface tension was then calculated for different contractions of the top layer in the $[01\bar{1}]$ direction. The results shown in fig. 5a indicate a 4% contraction in the $[01\bar{1}]$ direction to be most favourable, which defines a (1×5) superstructure. As can be inferred from table 2, the surface energies of the "top" and "bridge" registries are energetically nearly degenerate. The obtained slight preference of the "bridge" structure would require the support of a more sophisticated calculation. The calculated relaxations of the individual atoms, plotted in fig. 4b, show a "double maximum–double minimum"

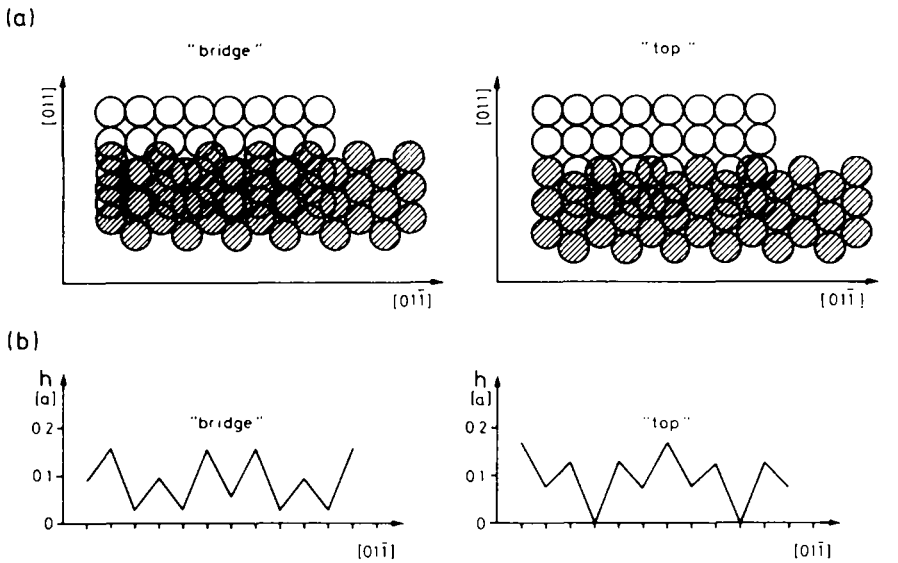

Fig. 4. (a) Structural models for the fcc(100)-(1 × 5) reconstruction in the "bridge" and "top" registry, as proposed in refs. [8,19]. The cross-hatched atoms belong to the hexagonal close-packed top layer. (b) Calculated vertical relaxations of individual atoms (in units of the lattice constant a) at fcc(100)-(1 × 5) surfaces in the "top" and "bridge" registry.

structure in the "bridge" registry and a "single maximum–single minimum" structure in the "top" registry, in agreement with the experiment [19].

Keeping the contraction in the [01$\bar{1}$] direction constant, the surface tension could further be decreased by allowing for a contraction in the [011] direction, yielding a 4% contraction as most favourable (fig. 5b). This (hex) reconstructed surface shows a coexistence of the "top" and "bridge" registries defined in the (1 × 5) structure [19]. Unlike for the contraction in the [01$\bar{1}$] direction, a small

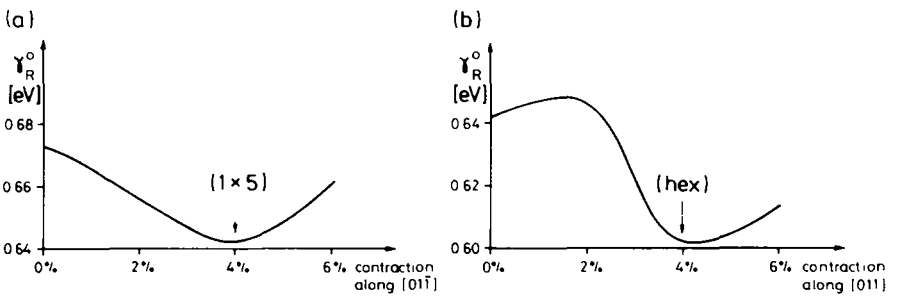

Fig. 5. The surface tension γ^0 at fcc(100) surfaces for different contractions (a) in the [01$\bar{1}$] direction and (b) in the [011] direction.

activation barrier has to be surmounted in the latter case in order to reach the (hex) structure with a 4% uniform contraction within the topmost layer. Note, such activation barriers are expected to exist between different hexagonal reconstruction phases. As can be seen from table 2, the heat of reconstruction (with respect to an unreconstructed surface with isolated adatoms) is $\Delta\gamma_R^0 = -0.09$ eV per surface atom in the (hex) phase and nearly -0.06 eV in the (1×5) phase.

3.4. CO chemisorption-suppressed Pt(100)-(hex) reconstruction

The property of some adsorbates to suppress reconstruction has been widely used also to prepare metastable unreconstructed surfaces [10,27]. It has been found experimentally that already very small coverages $\theta \gtrsim 0.05$ of CO suppress the (hex) reconstruction at Pt(100) surfaces [11]. This behaviour can be calculated by using eq. (4) and our reconstruction criterion, eq. (5). This is illustrated in fig. 1b. For metal adatoms, $\Delta\gamma^{ads}$ can be determined by calculating heats of adsorption from eq. (6) or its simple extension in the case that the adsorbate and substrate atom types are different [26]. Depending on the changes in adsorption geometry (coordination numbers, bond lengths) $\Delta\gamma^{ads}$ can be positive or negative. For nonmetallic adsorbates such as CO, NO, etc., where also charge transfers occur which cannot be reliably accounted for by a simple calculation, we estimate $\Delta\gamma^{ads}$ from experiment.

For the Pt(100) surface we use $\Delta\gamma_R^0 = -0.09$ eV. The adsorption energies have been given as [11] $E_{ads,R}(CO/Pt(100)) = 1.19$ eV and $E_{ads,U}(CO/Pt(100)) \gtrsim 1.63$ eV on the reconstructed and unreconstructed surface, respectively [30]. Using $\Delta\gamma^{ads} \gtrsim \theta \times 0.44$ eV in eq. (5), we find a critical coverage $\theta_{crit} \lesssim 0.2$ for the local suppression of reconstruction. This agrees very well with the observed value [11] $\theta_{crit} \approx 0.05$, which is an average coverage and neglects island formation.

3.5. H chemisorption-induced Ni and Pd(110)-(1×2) reconstruction

On hydrogen-covered (110) surfaces of Ni and Pd a large number of superstructures has been observed, which for coverages larger than $\theta_{crit}(H) = 1$ involved a (1×2) reconstruction of the substrate [12,15]. The paired rows model (see fig. 3a) has been suggested for this reconstruction [12], since it provides new adsorption sites for hydrogen atoms at $\theta > 1$. The proposed domain structure [12] accounts for streaks in the LEED pattern observed on Ni(110). Row pairing at the (110) surface also enables hydrogen to occupy subsurface sites on the Pd(110) surface at high coverages [15]. The effect of hydrogen to induce surface reconstruction is demonstrated in fig. 1a.

In our calculation for the hydrogen-induced reconstruction on Ni(110) we use for Ni $E_{coh}(bulk) = 4.46$ eV and use for simplicity the same p and q values

as in Pt [24]. We obtain the surface tensions $\gamma_U^0 = 1.40$ eV for the unreconstructed surface and $\gamma_R^0 = 2.05$ eV for the paired rows reconstructed surface (corresponding to surface areas shown in fig. 3a, and assuming d equal to the bulk nearest-neighbour distance). At clean Ni(110) surfaces the positive value $\Delta\gamma_R^0 = 0.65$ eV discards the paired rows reconstruction. In a second calculation we varied d in the range $0.6a \leqslant d \leqslant 1.0a$ (a being the lattice constant) and showed that $\Delta\gamma_R^0$ remains positive for all these pairing distances. Using for the hydrogen adsorption bond energy on the unreconstructed Ni(110) surface the observed value [31] $E_{ads,U}(H/Ni(110)) = 2.70$ eV (corresponding to the heat of adsorption of 0.93 eV), $\theta_{crit} = 1$ and the heat of reconstruction (per single surface atom of the unreconstructed surface) $\Delta\gamma_R^0 = 0.33$ eV, we conclude from eq. (5) that the average hydrogen adsorption bond energy must increase to $E_{ads,R}(H/Ni(110)) \gtrsim 3.03$ eV in order to induce reconstruction. Theoretically, we also expect an increased adsorption energy for hydrogen in subsurface sites of the reconstructed surface as a result of larger coordination. Note, the adsorption energies used in eq. (5) also include adsorbate-induced changes in the electronic structure and bonding of the substrate, which are likely to occur in the presence of hydrogen.

4. Discussion

We have shown that general trends observed for multilayer relaxations and reconstruction behaviour at transition metal surfaces can be quantitatively understood by using a fairly simple electronic model. Contractions of the topmost interlayer distance, and in some cases (at Pt, Ir and Au(100)-(hex) surfaces) in-plane contractions of the topmost layer, can be understood to arise due to the unsaturated coordination at surfaces.

Our results indicate that at fcc surfaces packing effects seem to be the driving force for reconstruction. While at bcc(100) surfaces the $(\sqrt{2} \times \sqrt{2})R45°$ superstructure of W is believed to be stabilized [22] by a half-filled surface state near E_F (no reconstruction is observed for the neighbouring Ta, where this state is empty [32]), this seems not to be the case at fcc surfaces. The very similar reconstruction behaviour at Ir, Pt and Au surfaces suggests that on late fcc metals details in the surface electronic structure are of minor importance for their reconstruction. This was already indicated by our earlier calculation of the Pt(110)-(1 × 2) reconstruction [28] yielding no surface states near E_F in Pt such as observed for W.

We conclude that mainly the close packing of the topmost layer (as observed at Ir, Pt and Au(100)-(hex) surfaces) is the driving force for reconstruction (see fig. 6). The decrease in the tension of the topmost layer, which is proportional to E_{coh}(bulk), is counteracted by a misregistry energy which depends on the shear modulus G. While both these effects have been consid-

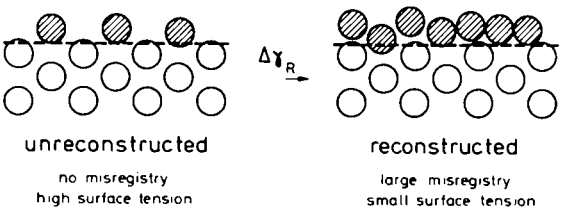

Fig. 6. Illustration of the decrease in surface free energy driving reconstruction. This is often achieved by close packing the topmost layer at the cost of misregistry with underlying layers.

ered in eqs. (1) and (6), it should be noted that G (and hence $\gamma^{(0)}$) have been underestimated [24] in eq. (6), which assumed all hopping integrals as isotropic. Generally, large values of G/E_{coh}(bulk) should suppress reconstruction, while small values facilitate reconstruction [34]. From the inspection of these data presented in table 3 it seems obvious, that clean 3d and 4d fcc metals do not spontaneously reconstruct in the same way as 5d metals do. Reconstruction on these surfaces can, however, be induced by even very small traces of adsorbates such as alkalis [13]. An improved discussion of the valency dependence of reconstruction and of the different behaviour of the 3d, 4d and 5d transition metals would require considering the angular dependence of the hopping integrals in eq. (6).

Concerning the surface multilayer relaxations, we calculate the equilibrium atomic positions by determining the global minimum of the surface tension in a multidimensional parameter space from eq. (7). In order to reach the global and not a local energy minimum, we adopted the following, physically plausible procedure. Starting from the unrelaxed surface, we first relaxed each layer, beginning with the topmost layer, and kept all other layers fixed during this relaxation. This calculation cycle through all layers has been repeated several times, until convergence was reached. In our opinion, this procedure correctly simulates relaxation processes at surfaces, where after cleavage at first only top-layer atoms relax due to their changed coordination.

Table 3
Ratio G/E_{coh}(bulk) for fcc transition metals (in 10^{28} m^{-3}); $G = C_{44}$ is used for the shear modulus [33] in the [100] direction on the (100) plane; $T = 0$ K

Co	Ni	Cu	↑ difficult
11.5	18.5	14.7	
Rh	Pd	Ag	reconstruction
?	11.4	10.8	
Ir	Pt	Au	↓ easy
24.1	8.2	7.4	

In summary, we calculated multilayer relaxations, surface energies and heats of reconstruction at clean and adsorbate-covered surfaces in such a way that general physical facts determining the surface geometry became apparent. The predicted oscillatory relaxations at fcc and bcc surfaces showed only a small material dependence and good quantitative agreement with experiment. Also the reconstruction trends predicted for clean fcc(110) and (100) surfaces agreed well with surface structures observed at Ir, Pt and Au surfaces. Deviations from this behaviour in the 3d and 4d metals have been accounted for by considering the ratio of the shear modulus and the bulk cohesive energy. A general criterion for adsorbate-suppressed and -induced reconstruction has been presented which describes properly the geometry of CO-covered Pt(100) and H-covered Ni(110) surfaces.

Note added in proof

We are grateful to Dr. W. Moritz for pointing out that the mechanism for the fcc(110)-$(1 \times 1) \rightleftarrows (1 \times 2)$ reconstruction described in section 3.2 accounts for structural changes observed on Au(110) surfaces [35]. A different "cross-channel" diffusion mechanism with site exchange has been proposed [36] and later observed [37] for the same reconstruction on Pt(110) surfaces. This mechanism, which has been studied intensively [38], assumes domain walls along the $[1\bar{1}0]$ direction. In contrast to the domain structure discussed in section 3.2, no low coordinated "edge" atoms exist and the domain wall energy is negligible in this case. Hence the local value of the heat of reconstruction (cf. table 2) $\Delta\gamma_R^{(1)} = -0.04$ eV applies to the surface as a whole. At higher temperatures, domain walls shown in fig. 3b become significant also in this system for the description of order–disorder transitions.

Acknowledgements

We gratefully acknowledge stimulating discussions with Professor K. Christmann, Dr. W. Moritz, Professor M.A. Van Hove, Professor K. Müller, Dr. G. Binnig and Dr. K.H. Rieder. This work was in part supported by the Deutsche Forschungsgemeinschaft, Sonderforschungsbereich 6.

References

[1] S.Y. Tsong, Phys. Today 37 (1984) 50.
[2] Y. Gauthier, R. Baudoing, Y. Joly, C. Gaubert and J. Rundgren, J. Phys. C17 (1984) 4547.
[3] D.L. Adams, H.B. Nielsen and J.N. Andersen, Phys. Scripta 27 (1983).
[4] Y. Kuk and L.C. Feldmann, Phys. Rev. B30 (1984) 5811.

[5] J.R. Noonan and H.L. Davis, Phys. Rev. B29 (1984) 4349.
[6] J.N. Andersen, H.B. Nielsen, L. Petersen and D.L. Adams, J. Phys. C17 (1984) 173.
[7] J. Sokolov, H.D. Shih, U. Bardi, F. Jona and P.M. Marcus, Solid State Commun. 48 (1983) 739.
[8] M.A. Van Hove, R.J. Koestner, P.C. Stair, J.P. Bibérian, L.L. Kesmodel, I. Bartoš and G.A. Somorjai, Surface Sci. 103 (1981) 189, 218.
[9] E. Lang, K. Müller, K. Heinz, M.A. Van Hove, R.J. Koestner and G.A. Somorjai, Surface Sci. 127 (1983) 347.
[10] K. Heinz, E. Lang, K. Strauss and K. Müller, Surface Sci. 120 (1982) L401.
[11] P.A. Thiel, R.J. Behm, P.R. Norton and G. Ertl, J. Chem. Phys. 78 (1983) 7448.
[12] K. Christmann, V. Penka, R.J. Behm, F. Chehab and G. Ertl, Solid State Commun. 51 (1984) 487.
[13] B.E. Hayden, K.C. Prince, P.J. Davie, G. Paolucci and A.M. Bradshaw, Solid State Commun. 48 (1983) 325.
[14] K.H. Rieder, T. Engel, R. Swendsen and M. Manninen, Surface Sci. 127 (1983) 223.
[15] K.H. Rieder, M. Baumberger and W. Stocker, Phys. Rev. Letters 51 (1983) 1799.
[16] I.K. Robinson, Phys. Rev. Letters 50 (1983) 1145.
[17] H. Niehus, Surface Sci. 145 (1984) 407.
[18] G. Binnig, H. Rohrer, Ch. Gerber and E. Weibel, Surface Sci. 131 (1983) L379.
[19] G.K. Binnig, H. Rohrer, Ch. Gerber and E. Stoll, Surface Sci. 144 (1984) 321.
[20] L.D. Marks, Phys. Rev. Letters 51 (1983) 1000.
[21] R.N. Barnett, U. Landmann and C.L. Cleveland, Phys. Rev. Letters 51 (1983) 1359, and references by these authors cited therein.
[22] I. Terakura, K. Terakura and N. Hamada, Surface Sci. 111 (1981) 479; 103 (1981) 103; D.W. Bullett and P.C. Stephenson, Solid State Commun. 45 (1983) 47.
[23] J. Ferrante, J.R. Smith and J.H. Rose, Phys. Rev. Letters 50 (1983) 1385; J.H. Rose, J. Ferrante and J.R. Smith, Phys. Rev. Letters 47 (1981) 675; J.H. Rose, J.R. Smith and J. Ferrante, Phys. Rev. B28 (1983) 1835.
[24] D. Spanjaard and M.C. Desjonquères, Phys. Rev. B30 (1984) 4822.
[25] D. Tománek, S. Mukherjee and K.H. Bennemann, Phys. Rev. B28 (1983) 665, and references cited therein; Phys. Rev. B29 (1984) 1076 (erratum).
[26] D. Tománek, A.A. Aligia and C.A. Balseiro, Phys. Rev. B, in press.
[27] H.P. Bonzel and S. Ferrer, Surface Sci. 118 (1982) L263, and references cited therein.
[28] D. Tománek, H.-J. Brocksch and K.H. Bennemann, Surface Sci. 138 (1984) L129.
[29] D. Tománek, submitted for publication.
[30] The more appropriate low-coverage value has been used for $E_{ads,U}$: the heat of adsorption decreases above θ_{crit} due to repulsive adsorbate interactions.
[31] K. Christmann, O. Schober, G. Ertl and M. Neumann, J. Chem. Phys. 60 (1974) 4528.
[32] A. Titov and W. Moritz, Surface Sci. 123 (1982) L709.
[33] Landolt–Börnstein, New Series, Vol. 11, Eds. K.H. Hellwege and A.M. Hellwege (Springer, Berlin, 1979).
[34] A similar criterion using the melting and Debye temperature is given in ref. [8].
[35] W. Moritz and D. Wolf, Surface Sci. 88 (1979) L29; H. Jagodzinski, W. Moritz and D. Wolf, Surface Sci. 77 (1978) 233; W. Moritz, H. Jagodzinski and D. Wolf, Surface Sci. 77 (1978) 249; D. Wolf, H. Jagodzinski and W. Moritz, Surface Sci. 77 (1978) 265, 283, and in preparation.
[36] D.W. Bassett and P.R. Webber, Surface Sci. 70 (1978) 520.
[37] J.D. Wrigley and G. Ehrlich, Phys. Rev. Letters 44 (1980) 661.
[38] S.H. Garofalani and T. Halicioglu, Surface Sci. 112 (1981) L775; 104 (1981) 199; 121 (1982) L535; H.P. Bonzel, Surface Sci. 121 (1982) L531.